



Determination of the Carbon-Saturated SiO₂-CaO-TiO_x Phase Diagram at 1773 K

Takashi Murata¹ · Katsunori Yamaguchi¹

Submitted: 22 April 2022 / in revised form: 21 August 2022 / Accepted: 25 August 2022 / Published online: 26 October 2022
© ASM International 2022

Abstract In the present work, a pyrometallurgical process is considered, in which platinum group metals (PGMs) from the hydrometallurgical residue containing mainly TiO₂ are concentrated in a metal phase with Cu as a collector, and TiO₂ is separated into the slag phase, with SiO₂ and CaO as fluxing agents. Efficient separation is thought to be possible only if the slag remains a homogenous liquid, with no solid phases present. In this study, the phase diagram of the SiO₂-CaO-TiO_x system equilibrated with graphite and CO gas at 1773 K was experimentally determined to find the liquid slag composition region with a large solubility of TiO_x. The results showed that at high TiO_x slag concentrations, a reaction occurred with the graphite crucible to form solid TiC. Additionally, the solubility of TiO_x in the slag increased as the ratio of mass%CaO/mass%SiO₂ decreased.

Keywords phase equilibria · precious metal smelting · pyrometallurgy · slag · titanium oxide

1 Introduction

The demand for platinum group metals (PGMs, which include Pd and Rh) has been increasing owing to growth in the manufacturing of industrial products that require them, such as catalysts.¹ There is a very high demand for PGM recycling because of the uneven distribution and scarcity of

mineral resources. In the hydrometallurgical process used for recycling, a residue containing TiO₂ is generated along with PGMs. In the present work, an additional pyrometallurgical process of residue treatment was considered in which PGMs are concentrated in the metal phase with Cu as the collector, while TiO₂ separates into the slag phase containing SiO₂ and CaO as fluxing agents.

Many studies have been conducted on titanium oxides in slag because of their relevance to the steel industry. Devries et al. and Muan measured the liquidus of the SiO₂-CaO-TiO₂ system.^{2,3} Mizoguchi and Ueshima reported on the phase diagram of the Ti₂O₃-CaO-Al₂O₃ system, Kang and Lee determined the phase diagram of the Fe-Al-Ti-O system, and Shi et al. studied the phase relations of the CaO-SiO₂-TiO₂-Al₂O₃-MgO system at 1250–1400 °C. Numerous researchers have investigated the oxidation state of Ti in slag.^{9–13} They reported that the percentage of Ti⁴⁺ decreases while the percentage of Ti³⁺ increases under the high-temperature reducing conditions typically encountered in steelmaking. Morizane et al. and Datta et al. reported on the formation of TiC in molten slag.^{10,14}

In the current work, a recycling process for PGMs is considered that uses graphite as the refractory of the furnace, which could possibly lead to the generation of solid phases such as TiC or TiO_x. Consequently, there is a concern that the presence of solid phases in the slag during melting will increase the viscosity of the slag, thereby preventing slag/metal separation and causing the loss of valuable metal to the slag. However, no study has reported on the equilibrium of carbon or TiC with Ti-containing slag. The goal of this study was to determine the slag composition region that remains liquid at a high C activity during this process. For this purpose, we attempted to experimentally determine the phase diagram of the SiO₂-CaO-TiO_x system containing TiC.

✉ Takashi Murata
tm2614971@akane.waseda.jp

¹ Department of Resources and Environmental Engineering, Waseda University, Okubo Shinjuku-ku, Tokyo, Japan

2 Experimental Procedure

A total of approximately 0.5 g of SiO₂, CaO calcined from CaCO₃, and TiO₂ (rutile-type) powder of special reagent grade was mixed according to the target composition and placed in a graphite crucible with an inner diameter of 8 mm. The sample was then inserted into a reaction tube with a CO (99.95 vol% purity) gas flow rate of 150 mL/min, held at 1773 K (± 3 K) in a furnace using SiC heating elements, then water quenched. By comparing results of samples held at temperature for 60 and 100 h in a preliminary experiment, it was determined that 60 h was sufficient to reach equilibrium. Therefore, all further experiments in this study were held for 60 h.

A schematic of the experimental setup is shown in Fig. 1. After quenching, the samples were embedded in ethyl acetate resin, polished, and sputter-coated with platinum. The compositions of the equilibrium phases were determined by scanning electron microscopy with energy-dispersive X-ray microanalysis (SEM-EDX; JOEL, JSM-6510A). The analytical setting for SEM-EDX was an accelerating voltage of 15 kV, and the obtained characteristic X-rays were corrected using the ZAF method. For the TiC formation experiment, the molar ratio of Ti to C in TiC was determined by electron probe microanalysis (EPMA; JOEL, JXA-8230) because the analytical accuracy of C is inferior in EDX. The analytical setting for EPMA was an accelerating voltage of 15 kV, and the obtained characteristic X-rays were corrected using the ZAF method. To ensure statistical reliability, at least five points were measured in each phase using SEM-EDX and EPMA. TiO₂, CaSiO₃, and C, which were coated with platinum under the same conditions as the experimental samples, were used as standard samples for EPMA. Additionally, the

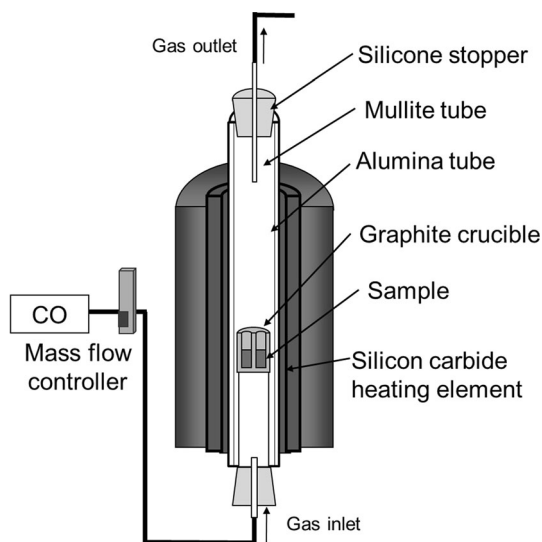


Fig. 1 Schematic of the experimental setup

equilibrium phases were identified by X-ray diffraction (XRD; RIGAKU, SmartLab) with Cu K α radiation.

3 Results and Discussion

Table 1 shows the initial composition, compositions of the equilibrium phases and compositional standard deviations of each sample. For the samples in which TiC was formed, Table 2 shows the results of quantitative analysis of the TiC phase, the compositional standard deviations, and the molar ratio of Ti to C. Because it is difficult to determine the concentration of O in EPMA from standard samples, the residue of the quantitative values for Ti, C, Si, and Ca was regarded as the concentration of O.

The back-scattered electron images obtained by SEM-EDX, and the diffraction patterns obtained by XRD are shown in Fig. 2–4. Figure 2(a) shows the back-scattered electron image of the sample in equilibrium with the liquid phase and SiO₂, and (b) shows the XRD results of this sample. Figure 3 and 4 present analogous results for equilibrium conditions involving (liquid + SiO₂ + TiC) and (liquid + TiC), respectively. From the results of SEM-EDX and EPMA, it was found that the TiC had oxygen in solid solution. Studies on titanium oxycarbide have also been published.^{15–20} Because the present experiments were conducted under conditions like those studies, it is likely that titanium oxide became titanium oxycarbide when the titanium activity was large. In this study, the ratio of C in the Ti and C rich phase ranged from 0.7 to 0.95, and the diffraction pattern was consistent with that of TiC by XRD, so it was TiC. Si, Ca, O detected in the TiC phase was either solid-solution in TiC or present in the surrounding slag because TiC phase is fine.

In the case of samples in which the liquid phase and CaSiO₃ were in equilibrium, clear back-scattered electron images that could differentiate the two phases could not be obtained, because the average mass numbers of the liquid phase and CaSiO₃ phase were very close. Therefore, for these samples, the liquidus composition was assumed to be midway between the initial composition of the sample in which CaSiO₃ was confirmed by XRD and the composition of the sample in which it became a homogeneous liquid.

In this experiment, we considered the degrees of freedom from the Gibbs phase rule. This rule is expressed by the following equation:

$$f = c - p + 2 \quad (\text{Eq 1})$$

where f is the degrees of freedom, c is the number of components, and p is the number of phases. In this study, $c = 5$ because the components are Si, Ca, Ti, C, and O. Therefore, there are seven maximum possible degrees of freedom. When the sample contained two solid phases

Table 1 Experimentally determined equilibrium phase compositions of the SiO₂-CaO-Ti₃O₅ system containing TiC equilibrated with graphite and CO gas at 1773 K (Carbon-saturated, $p_{CO} = 1$)

No	Initial composition/mass%			Phase	Equilibrium phase composition/mass%		
	SiO ₂	CaO	TiO ₂		SiO ₂	CaO	Ti ₃ O ₅
1	73.00	27.00	0.00	Liquid	68.8 ± 0.48	31.2 ± 0.48	...
				SiO ₂	99.9 ± 0.09	0.1 >	...
2	68.75	25.91	5.34	Liquid	65.3 ± 0.38	28.5 ± 0.21	6.2 ± 0.31
				SiO ₂	99.7 ± 0.19	0.1 ± 0.06	0.2 ± 0.13
3	59.24	21.72	19.04	Liquid	57.5 ± 0.48	22.9 ± 0.41	19.6 ± 0.70
				SiO ₂	99.4 ± 0.23	0.1 >	0.5 ± 0.27
4	55.96	16.69	27.35	Liquid	53.8 ± 1.21	21.6 ± 0.76	24.6 ± 0.74
				SiO ₂	99.2 ± 0.24	0.1 ± 0.13	0.7 ± 0.26
5	54.86	14.70	30.44	Liquid	53.0 ± 0.98	22.5 ± 1.17	24.5 ± 0.50
				SiO ₂	99.0 ± 0.23	0.2 ± 0.21	0.7 ± 0.18
				TiC			
6	55.21	23.66	21.13	Liquid	59.4 ± 0.48	27.1 ± 0.18	13.5 ± 0.54
				TiC			
7	52.29	27.62	20.09	Liquid	60.8 ± 0.44	26.2 ± 0.39	13.0 ± 0.50
				TiC			
8	53.46	31.68	14.85	Liquid	58.3 ± 0.24	35.0 ± 0.36	6.7 ± 0.38
				TiC			
9	51.56	35.69	12.75	Liquid	54.5 ± 0.26	40.5 ± 0.61	5.0 ± 0.55
				TiC			
10	41.55	42.54	15.90	Liquid	53.0 ± 0.41	42.4 ± 0.47	4.6 ± 0.28
				TiC			
11	41.41	37.46	21.13	Liquid	50.5 ± 0.22	45.9 ± 0.34	3.6 ± 0.24
				TiC			
12	36.61	47.49	15.90	Liquid	46.7 ± 1.01	51.1 ± 1.55	2.1 ± 0.66
				TiC			
				Ca ₂ SiO ₄	38.0 ± 0.54	61.4 ± 0.54	0.6 ± 0.19
13	37.89	57.83	4.27	Liquid	45.7 ± 0.31	52.0 ± 0.26	2.3 ± 0.10
				Ca ₂ SiO ₄	37.3 ± 0.32	62.1 ± 0.46	0.6 ± 0.26
14	49.57	49.57	0.86	Liquid			
				CaSiO ₃			
15	52.57	46.57	0.86	Liquid			
				CaSiO ₃			
16	62.42	23.78	13.80	Liquid	58.6 ± 0.32	36.1 ± 0.58	5.4 ± 0.37
17	47.93	49.93	2.14	Liquid	51.8 ± 0.23	46.5 ± 0.37	1.7 ± 0.44
18	52.92	44.94	2.14	Liquid	49.5 ± 0.45	48.9 ± 0.48	1.6 ± 0.10

Table 2 Compositions of TiC in equilibrium with the liquid phase at 1773 K

No	Composition of TiC, mol%					Molar ratio Ti:C
	Ti	C	Si	Ca	O	
5	43.37 ± 4.96	30.30 ± 4.14	3.28 ± 2.17	1.99 ± 1.28	21.06 ± 4.83	1:0.70
6	43.13 ± 4.46	38.01 ± 3.70	3.42 ± 1.83	2.13 ± 0.97	13.31 ± 5.22	1:0.88
7	38.70 ± 5.19	30.76 ± 7.17	5.44 ± 2.28	2.65 ± 1.04	22.45 ± 8.20	1:0.79
8	44.31 ± 3.97	40.15 ± 3.99	2.70 ± 1.69	2.11 ± 1.24	10.74 ± 4.78	1:0.91
9	49.31 ± 1.95	44.79 ± 1.55	0.86 ± 0.74	1.03 ± 0.61	4.01 ± 1.80	1:0.91
10	48.78 ± 2.25	44.24 ± 3.03	0.60 ± 0.52	0.86 ± 0.47	5.52 ± 3.85	1:0.91
11	48.42 ± 1.31	46.12 ± 3.09	0.69 ± 0.60	0.95 ± 0.64	3.82 ± 2.54	1:0.95
12	51.32 ± 0.41	43.65 ± 1.96	0.12 ± 0.05	1.01 ± 0.07	3.90 ± 1.75	1:0.85

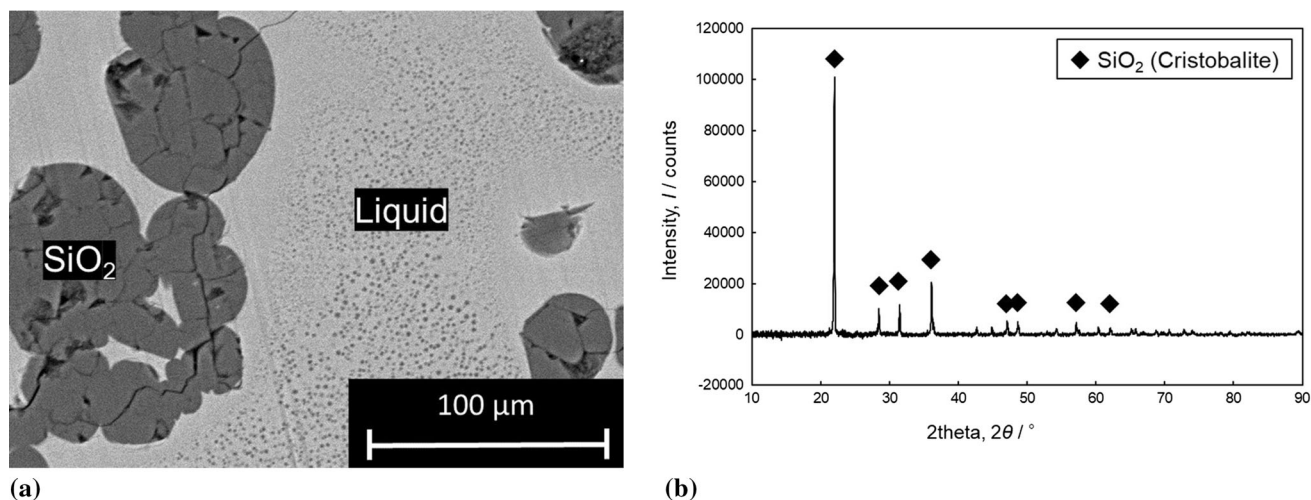


Fig. 2 Equilibrium with the liquid phase and SiO_2 ; (a) back-scattered electron image, and (b) diffraction pattern

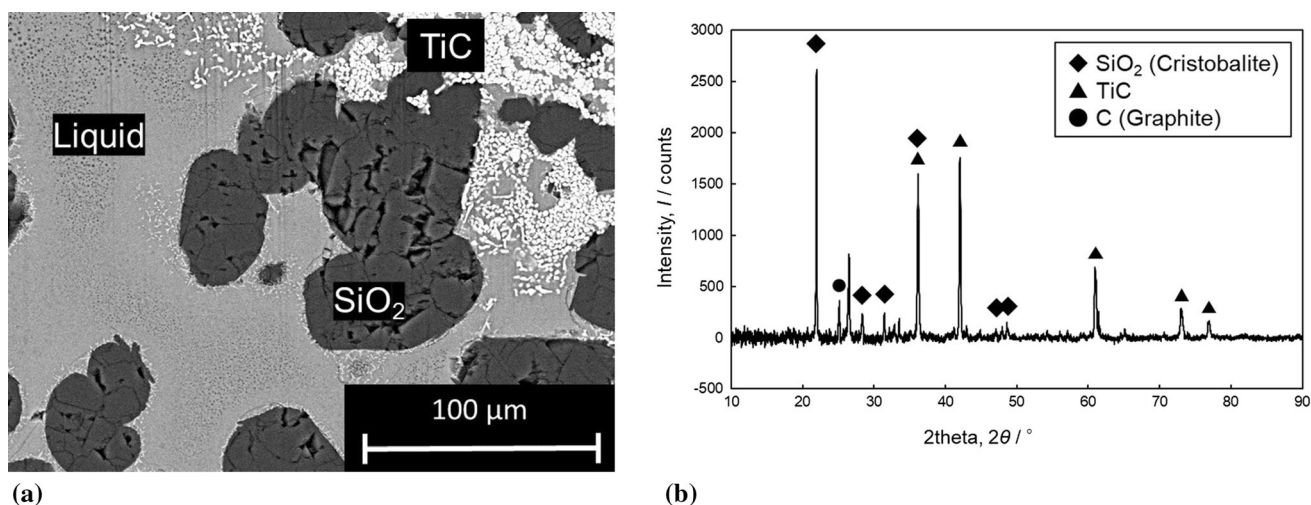
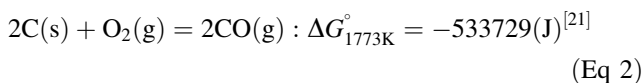


Fig. 3 Equilibrium with the liquid phase, SiO_2 , and **TiC**; (a) back-scattered electron image, and (b) diffraction pattern

different from the liquid phase, in addition to the gas phase and the graphite crucible, $p = 5$ and $f = 2$. When a gas phase at a pressure of 1 atm and a temperature of 1773 K are specified, $f = 0$ and the composition of the liquid phase is fixed. Thus, in this experimental system, the equilibrium compositions of the three phases do not change in the three-phase region.

In this study, we considered the p_{O_2} and the oxidation state of Ti. From thermodynamic calculations, when the $a_c = 1$ and the CO partial pressure ($p_{\text{CO}} = 1$ at 1773 K, $p_{\text{O}_2} = 10^{-15.7}$. The reaction is expressed as follows:



In this study, the oxidation state of Ti in the liquid slag phase was not determined. According to the thermodynamics of the Ti-O binary system, Ti_3O_5 is the most

stable form of titanium oxide at $p_{\text{O}_2} = 10^{-15.7}$ and a temperature of 1773 K.⁷ Additionally, under similar conditions, it has been reported that the value of $\text{Ti}^{3+}/\text{Ti}^{4+}$ in the slag becomes smaller as the slag basicity or p_{O_2} increases.^{9–13} Considering these factors, the composition of the liquid phase was calculated from the concentrations determined for each of the metallic elements by SEM-EDX analysis, assuming that Ti in the liquid phase exists entirely as Ti_3O_5 . The resulting phase diagram of the SiO_2 -CaO- TiO_x system containing **TiC** is shown in Fig. 5. This figure shows that as the basicity ($\text{mass}\%\text{CaO}/\text{mass}\%\text{SiO}_2$) decreases, **TiC** becomes less stable and more Ti_3O_5 dissolves in the slag. These phenomena show that the decrease in the slag basicity leads to the decrease of TiO_x activity.

Because Si, Ca, and O are soluble in solid **TiC** as shown in Table 2, **TiC** is not a pure substance, although $a_{\text{TiC}} = 1$ is assumed. In this case, the **TiC**-equilibrated liquidus line

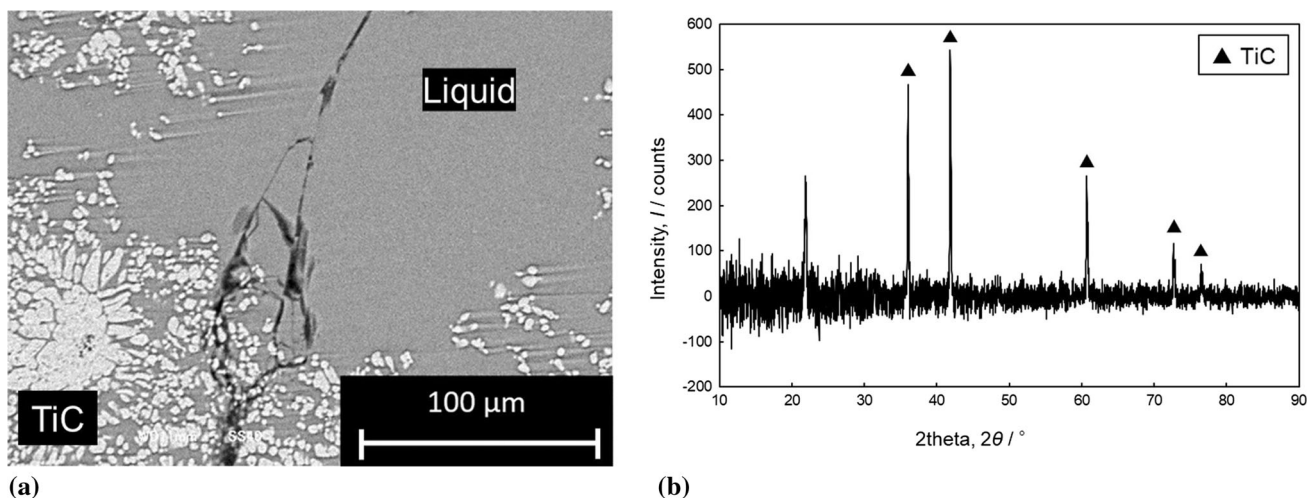


Fig. 4 Equilibrium with the liquid phase and TiC; (a) back-scattered electron image, and (b) diffraction pattern

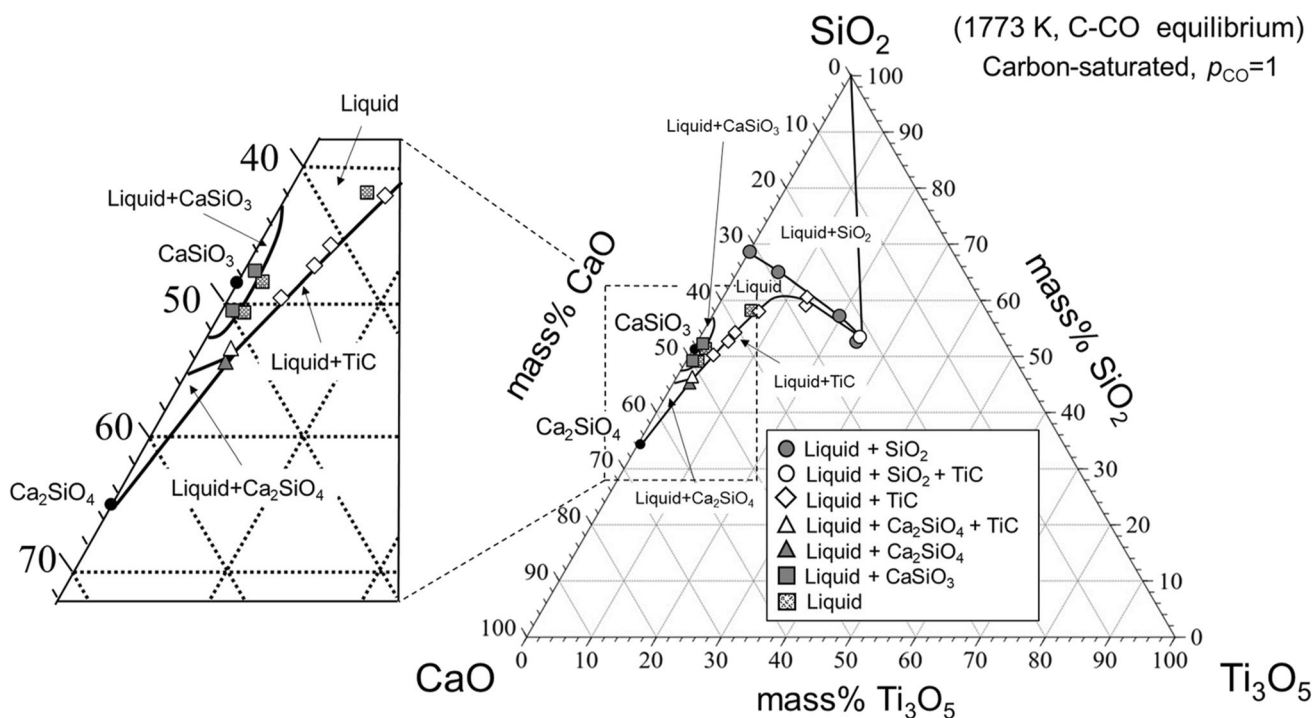
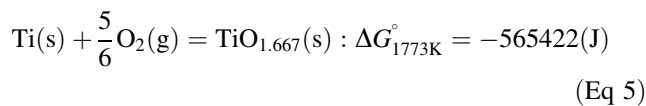
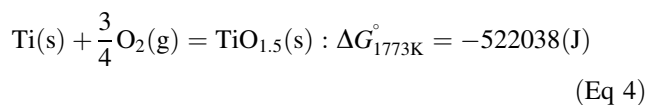
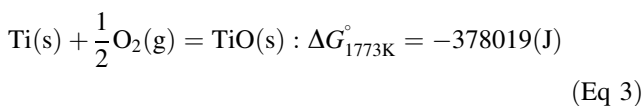
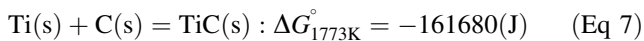
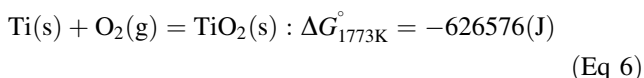


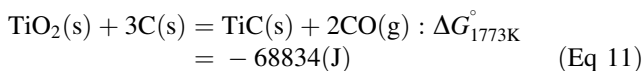
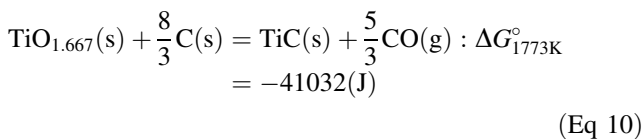
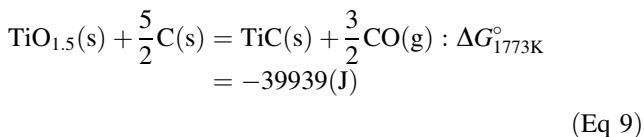
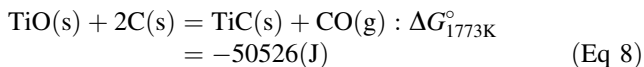
Fig. 5 Phase diagram of the SiO₂-CaO-Ti₃O₅ system containing TiC equilibrated with graphite and CO gas at 1773 K (Carbon-saturated, $p_{CO} = 1$)

can be regarded as an isoactivity line of TiO_x in the slag. The activity of TiO_x in this experiment was calculated using the FTdemoBASE of FactSage database.²¹ The Gibbs free energies of the reactions for the formation of typical titanium oxides and TiC are as follows:





Using the reactions (3) to (7), the reactions of these titanium oxides with carbon are as follows:



From these reactions, the activity of TiO_x on the liquidus line equilibrated with solid TiC at $a_{\text{C}} = 1$, $a_{\text{TiC}} = 1$, and $p_{\text{CO}} = 1$ at 1773 K were derived as $a_{\text{TiO(s)}} = 0.0325$, $a_{\text{TiO}_{1.5}(\text{s})} = 0.0666$, $a_{\text{TiO}_{1.667}(\text{s})} = 0.0618$, and $a_{\text{TiO}_2(\text{s})} = 0.00938$, respectively. The calculation results suggest that solid TiC is formed under the conditions of higher concentration of titanium oxide and high carbon activities, presumably leading to potential problems with slag/metal separation and efficiency of the proposed recycling process. It is thought that TiC formation can be suppressed by avoiding the use of graphite crucibles and reducing the carbon activity, for example, by using a SiC crucible.

4 Conclusion

The phase diagram of the C and CO-saturated SiO_2 -CaO- TiO_x system containing TiC was prepared by the quenching method at 1773 K. The solubility of TiO_x in the slag increased as the slag basicity decreased, and in the case of high TiO_x activity, TiO_x was reduced by C to form TiC. To form a slag with higher titanium solubility, the use of graphite crucibles should be avoided, and carbon activity should be reduced, for example, by using a SiC crucible.

Acknowledgments The authors would like to thank Tanaka Kikinzoku Kogyo K.K. for their helpful suggestions and discussions, Kagami Memorial Research Institute for Materials Science and Technology of Waseda University for the use of XRD and EPMA, and Editage (www.editage.com) for language support during the preparation of this paper.

References

- D. Xun, H. Hao, X. Sun, Z. Liu, and F. Zhao, End-of-Life Recycling Rates of Platinum Group Metals in the Automotive Industry: Insight into Regional Disparities, *J. Clean. Prod.*, 2020. <https://doi.org/10.1016/j.jclepro.2020.121942>
- R.C. Devries, R. Roy, and E.F. Osborn, Phase Equilibria in the System CaO-TiO₂-SiO₂, *J. Am. Ceram.*, 1955, **38**, p 158–171. <https://doi.org/10.1111/j.1151-2916.1955.tb14922.x>
- A. Muan, Equilibrium Relations Involving Transition-Metal Oxides at High Temperatures, *Adv. Ceram.*, 1990, **3**, p 25–44.
- T. Mizoguchi, and Y. Ueshima, Determination of the Ti₂O₃-CaO-Al₂O₃ Phase Diagram at Steelmaking Temperature, *Tetsu-to-Hagane*, 2005, **91**, p 376–382. https://doi.org/10.2355/tetsuohagane1955.91.4_376, (in Japanese)
- Y. Kang, and J. Lee, Reassessment of Oxide Stability Diagram in the Fe-Al-Ti-O System, *ISIJ Int.*, 2017, **57**, p 1665–1667. <https://doi.org/10.2355/isijinternational.ISIJINT-2017-182>
- J. Shi, M. Chen, X. Wan, P. Taskinen, and A. Jokilaakso, Phase Equilibrium Study of the CaO-SiO₂-MgO-Al₂O₃-TiO₂ System at 1300°C and 1400°C in air, *JOM*, 2020. <https://doi.org/10.1007/s11837-020-04136-1>
- X. Wan, J. Shi, L. Klemettinen, M. Chen, P. Taskinen, and A. Jokilaakso, Equilibrium Phase Relations of CaO-SiO₂-TiO₂ System at 1400 °C and Oxygen Partial Pressure of 10–10 atm, *J. Alloys Compd.*, 2020, **847**, p 156472. <https://doi.org/10.1016/j.jallcom.2020.156472>
- M. Chen, J. Shi, P. Taskinen, and A. Jokilaakso, Phase Equilibria of the CaO-SiO₂-TiO₂-Al₂O₃-MgO System in Air at 1250–1400 °C, *Ceram. Int.*, 2020, **46**, p 27702–27710. <https://doi.org/10.1016/j.ceramint.2020.07.268>
- S.K. Panda, and I. Jung, Coupled Experimental Study and Thermodynamic Modeling of the Al₂O₃-Ti₂O₃-TiO₂ System, *ISIJ Int.*, 2020, **60**, p 31–41. <https://doi.org/10.2355/isijinternational.ISIJINT-2019-006>
- Y. Morizane, B. Ozturk, and R.J. Fruehan, Thermodynamics of TiO_x in Blast Furnace-type Slags, *Metall. Mater. Trans. B*, 1999, **30**, p 29–43. <https://doi.org/10.1007/s11663-999-0004-y>
- G. Tranell, O. Ostrovski, and S. Jahanshahi, The Equilibrium Partitioning of Titanium Between Ti₃₊+ and Ti₄₊+ Valency States in CaO-SiO₂-TiO_x slags, *Metall. Mater. Trans. B*, 2002, **33**, p 61–67. <https://doi.org/10.1007/s11663-002-0086-2>
- C. Ariyo, P. Gonzalez, and L. Holappa, Oxidation state of Titanium in CaO-SiO₂-TiO_x Slags at 1873K, *Steel Res. Int.*, 2005, **76**, p 284–287. <https://doi.org/10.1002/srin.200506010>
- S. Jung, and R.J. Fruehan, Thermodynamics of Titanium Oxide in Ladle Slags, *ISIJ Int.*, 2001, **41**, p 1447–1453. <https://doi.org/10.2355/isijinternational.41.1447>
- K. Datta, P.K. Sen, S.S. Gupta, and A. Chatterjee, Effect of Titania on the Characteristics of Blast Furnace Slags, *Steel Res. Int.*, 1993, **64**, p 232–238. <https://doi.org/10.1002/srin.199301015>
- A. Ouensanga, Thermodynamics of the Ti-C-O System at 1580 K, *J. Less Common Met.*, 1981, **79**, p 237–241. [https://doi.org/10.1016/0022-5088\(81\)90072-2](https://doi.org/10.1016/0022-5088(81)90072-2)
- Y. Hashimoto, K. Koyama, K. Suzuki, and A. Nanyoshi, Determination of Standard Gibbs Free Energy of Formation of Ti_xC_yO_z in Equilibrium with Carbon, *J. Jpn Inst. Met.*, 1989, **53**, p 1229–1235. https://doi.org/10.2320/jinstmet1952.53.12_1229, (in Japanese)
- M. Razavi, M.R. Rahimpour, and R. Kaboli, Synthesis of TiC nanocomposite Powder from Impure TiO₂ and Carbon Black by Mechanically activated Sintering, *J. Alloys Compd.*, 2008, **460**, p 694–698. <https://doi.org/10.1016/j.jallcom.2007.06.080>
- X. Meng, D. Liu, X. Dai, H. Pan, X. Wen, L. Zuo, and G. Qin, Novel Stable Hard Transparent Conductors in TiO₂-TiC System:

- Design Materials from Scratch, *Sci. Rep.*, 2014, **4**, p 1–7. <https://doi.org/10.1038/srep07503>
19. J. Dang, F. Fatollahi-Fard, P.C. Pistorius, and K. Chou, Synthesis of Titanium Oxycarbide from Titanium Slag by Methane-Containing Gas, *Metall. Mater. Trans. B*, 2018, **49**, p 123–131. <https://doi.org/10.1007/s11663-017-1123-5>
 20. G. Fan, J. Tan, R. Zhang, J. Dang, C. Bai, H. Lei, and C. Tan, Crystallization and Carbonization of TiO₂-CaO-SiO₂ Ternary Slag, *Energy Technol.*, 2020. https://doi.org/10.1007/978-3-030-36830-2_32
 21. C.W. Bale, E. Bélisle, P. Chartrand, S.A. Deckerov, G. Eriksson, A.E. Gheribi, K. Hack, I.H. Jung, Y.B. Kang, J. Melançon, A.D. Pelton, S. Petersen, C. Robelin, J. Sangster, P. Spencer, and M.-A. Van Ende, FactSage Thermochemical Software and Databases, 2010–2016, *Calphad*, 2016, **54**, p 35–53. <https://doi.org/10.1016/j.calphad.2016.05.002>

Publisher's Note Springer Nature remains neutral with regard to jurisdictional claims in published maps and institutional affiliations.